

Disturbance Rejection Control for Autonomous Trolley Collection Robots with Prescribed Performance

Rui-Dong Xi¹, Liang Lu¹, Xue Zhang¹, *Member, IEEE*, Xiao Xiao^{1,3}, *Member, IEEE*, Bingyi Xia¹, Jiankun Wang^{1,2}, *Senior Member, IEEE*, and Max Q.-H. Meng¹, *Fellow, IEEE*

Abstract—Trajectory tracking control of autonomous trolley collection robots (ATCR) is an ambitious work due to the complex environment, serious noise and external disturbances. This work investigates a control scheme for ATCR subjecting to severe environmental interference. A kinematics model based adaptive sliding mode disturbance observer with fast convergence is first proposed to estimate the lumped disturbances. On this basis, a robust controller with prescribed performance is proposed using a backstepping technique, which improves the transient performance and guarantees fast convergence. Simulation outcomes have been provided to illustrate the effectiveness of the proposed control scheme.

Index Terms—Skid-steered mobile robot, disturbance observer, prescribed performance control.

I. INTRODUCTION

THE deployment of robot systems to achieve autonomous recycling luggage trolleys is of great significance for increasing reuse efficiency of luggage trolleys, lowering labor expenses, and building a smart airport [1], [2]. However, this is an extremely difficult task since the extensive and intricate pedestrian flow poses great challenges to the perception, planning, and control of the autonomous trolley collection robots (ATCR) [3], [4]. In the research work of [2], an overall diagram of a differential steered ATCR is introduced and a model predictive controller (MPC) is developed as the preliminary control scheme, but the external disturbances and convergence rate are not fully considered. Hence, in this work, a disturbance rejection control scheme with prescribed performance is developed for robust and accurate control of the ATCR.

For an ATCR, there are some challenging problems that existed for example: i) the robot needs to travel effectively

in crowded and cramped environments; ii) the robot needs to dispose of skidding and slipping effectively under different road conditions, like slippery ground. In addition, while transporting a chain of collected luggage trolleys, two ATCRs have to collaborate with each other. As a consequence, the control system is required to have fast response, high precision, and high interference cancellation abilities.

To date, various control methods have been adopted in mobile robots for the sake of robust and precise trajectory tracking [5]–[7]. In the reference [5] and [8], second order sliding mode controllers are utilized, and in [6], a robust control scheme is developed for skid-steered mobile robots on account of challenging terrains. These methods have improved the robot’s resistance to skidding and slipping to a certain extent, and have compared different ground conditions. However, these commonly used methods are excessively dependent on the dynamics model and the accurate force between the robot and the ground. In practice, it is very difficult to accurately describe the dynamics model, and the force between the robot and the ground is constantly fluctuating with the change in the environment. Therefore, there exist significant model uncertainties and interference, and these factors have not been fully addressed.

Disturbance observer (DOB) is an efficient method to tackle model uncertainties and disturbances [9]–[14]. In the literature [9], Chen utilized a DOB to deal with the skidding, slipping, and input disturbances in a differential steering mobile robot. In [10] a fuzzy DOB is also utilized in the control of a differential steering mobile robot with skidding and slipping phenomenon. Nevertheless, the convergence rate has never been considered in these DOBs. Adaptive sliding mode disturbance observer (ASMDOB) as a new kind of DOB has been successfully developed to estimate lumped uncertainties in various electromechanical systems [15]–[17]. For instance, in the research works [18], [19] and [20], different ASMDOBs were introduced in the control of robot manipulators. In these works, in addition to the accurate observation of interference, fast convergence could also be guaranteed. In [20], the backstepping technique is initially utilized in the design of the ASMDOB. In this work, except for the fast and accurate observation of the lumped disturbances, the tracking cost has also been reduced and the

This work was supported by Shenzhen Key Laboratory of Robotics Perception and Intelligence (ZDSYS20200810171800001), Southern University of Science and Technology, Shenzhen 518055, China. (Corresponding authors: Max Q.-H. Meng.)

Rui-Dong Xi, Liang Lu, Xue Zhang, Xiao Xiao, Jian-Kun Wang and Max Q.-H. Meng are with Shenzhen Key Laboratory of Robotics Perception and Intelligence, the Department of Electronic and Electrical Engineering, Southern University of Science and Technology, Shenzhen 518055, China. (e-mail: max.meng@ieee.org).

Jiankun Wang is also with Jiaying Research Institute, Southern University of Science and Technology, Jiaying, China

Xiao Xiao is also with Yuanhua Robotics, Perception & AI Technologies Ltd. Shenzhen 518055, China.

engineering applicability has been further improved.

In addition to interference cancellation, transient performance like overshoot and convergence rate should also be considered in the controller design of ATCRs. Exactly, the prescribed performance control (PPC) is an effective way to solve this problem [21]–[23]. For example, in [23], an event-based PPC is investigated for control of dynamic positioning vessels with unknown and time-varying sea loads.

Inspired by the aforementioned discussions, an ASMDOB based robust controller with prescribed performance is developed in this study. Instead of using the complicated dynamics model, the kinematics model is adopted which guarantees the simplicity and applicability of the algorithm. The advantages of ASMDOB, backstepping technique, and PPC method are integrated in this controller. The main contributions of this work can be summarized as follows:

- A kinematics model based ASMDOB with fast convergence is proposed, which has the advantage of higher engineering practicability.
- A robust controller is developed integrating the PPC, backstepping technique, and finite-time convergence method. The proposed control scheme can not only ensure the fast convergence of tracking errors, but also guarantee transient performance.

Notation: In this brief, $\|\cdot\|$ represents the Euclidean norm. The vectors $\text{sgn}(\sigma) = [\text{sgn}(\sigma_1), \dots, \text{sgn}(\sigma_n)]^T$, $\text{sgn}^a(\sigma) = [|\sigma_1|^a \text{sgn}(\sigma_1), \dots, |\sigma_n|^a \text{sgn}(\sigma_n)]^T$.

II. PROBLEM STATEMENT

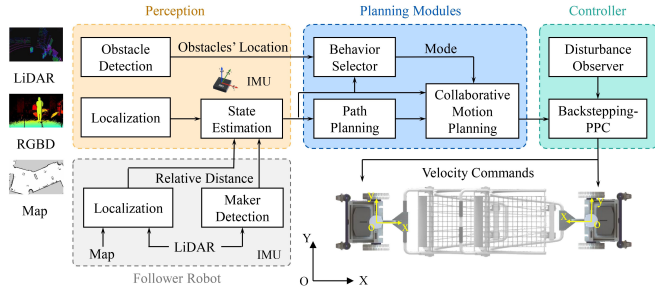


Fig. 1. Control system block diagram of the ATCR.

Overall control system block diagram of the developed ATCR is depicted in Fig. 1. This work mainly focus on the controller design. Define XOY as the fixed frame and xoy as a body frame, considering kinematics interference, kinematics model of the robot is given by

$$\dot{q} = Tu + d_v \quad (1)$$

where $q = [x \ y \ \theta]^T$, x and y denote the center point position corresponding to the fixed frame and θ is the robot's orientation, $u = [v \ \omega]^T$ presents the linear and angular velocity of the robot, and $T = \begin{bmatrix} \cos \theta & 0 \\ \sin \theta & 0 \\ 0 & 1 \end{bmatrix}$.

$d_v = [d_{vx} \ d_{vy} \ d_\omega]^T$ with d_{vx} , d_{vy} , d_ω present the velocity interference respectively.

The main objective of this work is to design an active disturbance rejection control scheme for the ATCR with both the transient and steady state performances guaranteed. To proceed with the design of control scheme, the following assumption and lemmas are required:

Assumption 1: The lumped interference d_v and its derivative are unknown but bounded.

Lemma 1 (see [20]): For positive definite function $V(t)$ which fulfills:

$$\dot{V}(t) + \kappa_1 V(t) + \kappa_2 V^\gamma(t) \leq 0, \forall t > t_0 \quad (2)$$

then $V(t)$ will converge to the equilibrium point in finite time t_s with

$$t_s \leq t_0 + \frac{1}{\kappa_1(1-\gamma)} \ln \frac{\kappa_1 V^{1-\gamma}(t_0) + \kappa_2}{\kappa_2} \quad (3)$$

where κ_1 , κ_2 , and γ are design parameters with $\kappa_1 > 0$, $\kappa_2 > 0$, $0 < \gamma < 1$.

Lemma 2 (see [9] and [20]): For the bounded initial conditions, if the Lyapunov function $V(x)$ satisfies $V_1(\|x\|) \leq V(x) \leq V_2(\|x\|)$ such that

$$\dot{V}(x) \leq -c_1 V(x) + c_2 \quad (4)$$

where $V_1, V_2: \mathbb{R}^n \rightarrow \mathbb{R}$ are class K functions and c_1, c_2 are positive constants, then the state $x(t)$ is uniformly bounded.

III. DESIGN OF THE OBSERVER BASED KINEMATICS CONTROLLER

A. Design of ASMDOB

In this part, the ASMDOB is introduced to estimate the uncertain part d_v in the kinematics model. At first, auxiliary variables $\sigma \in \mathbb{R}^{3 \times 1}$ and $z \in \mathbb{R}^{3 \times 1}$ are developed to reflect the system states as

$$\sigma = z - q. \quad (5)$$

Considering the function candidate $L_1 = \frac{1}{2} \sigma^T \sigma$ and derivative it with respect to time, one has

$$\dot{L}_1 = \sigma^T (\dot{z} - Tu - d_v). \quad (6)$$

Define

$$\dot{z} = Tu - c_1 \sigma - c_2 \text{sgn}^{\alpha_1}(\sigma) - k_d \text{sgn}(\sigma) \quad (7)$$

where c_1 , c_2 and k_d are positive design parameters and $0 < \alpha_1 < 1$. Substituting \dot{z} into (6) yields

$$\dot{L}_1 = -c_1 \sigma^T \sigma - c_2 \sigma^T \text{sgn}^{\alpha_1}(\sigma) - \sigma^T d_v - k_d \sigma^T \text{sgn}(\sigma). \quad (8)$$

While k_d is selected fulfills $k_d \geq \max \|\bar{d}_v\|$ ($\bar{d}_v \in \mathbb{R}^{3 \times 1}$ denotes the maximum interference in each directions), it is easy to obtain

$$\dot{L}_1 \leq -c_1 \sigma^T \sigma - c_2 \sigma^T \text{sgn}^{\alpha_1}(\sigma) \leq 0. \quad (9)$$

Then we have

$$\dot{L}_1 + 2c_{\min} L_1 + 2^{(1+\alpha_1)/2} c_{\min} L_1^{(1+\alpha_1)/2} \leq 0 \quad (10)$$

where $c_{\min} = \min\{c_1, c_2\}$. According to lemma 1, it can be concluded that z will converge to q in finite time. However, it can be seen in (7) that the variable structure term $k_d \text{sgn}(\sigma)$ will greatly influence the convergent performance due to its discontinuous characteristics. As a result, a low pass filter is adopted as

$$\lambda_0 \dot{\zeta} + \zeta = \mu \quad (11)$$

where $\mu = -c_1 \sigma - c_2 \text{sgn}^{\alpha_1}(\sigma) - k_d \text{sgn}(\sigma)$, λ_0 is the design parameter of the filter.

Define $s = \dot{\sigma} + \lambda_1 \sigma$ and the ASMDOB is devised as

$$\dot{\hat{d}}_v = \lambda_2 (\zeta + \lambda_1 \sigma - \hat{d}_v) - (k_s + \hat{\beta}) \text{sgn}(s) \quad (12)$$

where λ_1 , λ_2 and k_s are design parameters and $\hat{\beta}$ is the estimation of β as the upper bound of $\dot{\hat{d}}_v$. From (12) we can obtain

$$\dot{\tilde{d}}_v \doteq -\lambda_2 s - \lambda_2 \tilde{d}_v - (k_s + \hat{\beta}) \text{sgn}(s) + \dot{d}_v \quad (13)$$

where $\tilde{d}_v = d_v - \hat{d}_v$.

Theorem 1: For the kinematics model of the skid steered mobile robot (1), the ASMDOB is developed as in (12), while the observer gains are designed fulfills $\lambda_2 > 0$ and $k_s \geq \lambda_2 \|s - \tilde{d}_v\|$, and the adaptive law is given by

$$\dot{\hat{\beta}} = -\lambda_3 \hat{\beta} + \|s\| \quad (14)$$

where λ_3 is a positive parameter. Then the estimation error of the uncertainty \tilde{d}_v is uniformly bounded with exponentially convergent characteristics.

Proof: Considering the Lyapunov function

$$L_2 = \frac{1}{2} \tilde{d}_v^T \tilde{d}_v + \frac{1}{2} \tilde{\beta}^2 \quad (15)$$

where $\tilde{\beta} = \beta - \hat{\beta}$. The time derivative of L_2 is calculated as

$$\begin{aligned} \dot{L}_2 &= \tilde{d}_v^T \left[-\lambda_2 s - \lambda_2 \tilde{d}_v - (k_s + \hat{\beta}) \text{sgn}(s) + \dot{d}_v \right]^T + \tilde{\beta} \dot{\tilde{\beta}} \\ &= -2\lambda_2 \tilde{d}_v^T \tilde{d}_v - \lambda_2 \tilde{d}_v^T (s - \tilde{d}_v) - k_s \tilde{d}_v^T \text{sgn}(s) \\ &\quad - \hat{\beta} \tilde{d}_v^T \text{sgn}(s) + \tilde{d}_v^T \dot{d}_v - \tilde{\beta} \dot{\tilde{\beta}} \end{aligned} \quad (16)$$

According to the convergent property of σ and the equivalent output injection principle [24], it is observed that s can be concieved as the equivalent value of \tilde{d}_v . When the value of k_s is properly defined, we can obtain

$$\begin{aligned} \dot{L}_2 &\leq -2\lambda_2 \tilde{d}_v^T \tilde{d}_v - \hat{\beta} \|\tilde{d}_v^T\| + \tilde{d}_v^T \dot{d}_v - \tilde{\beta} \dot{\tilde{\beta}} \\ &\leq -2\lambda_2 \tilde{d}_v^T \tilde{d}_v + \tilde{\beta} \|\tilde{d}_v^T\| - \tilde{\beta} \dot{\tilde{\beta}} \\ &\leq -2\lambda_2 \tilde{d}_v^T \tilde{d}_v + \lambda_3 \tilde{\beta} \dot{\tilde{\beta}} \\ &\leq -2\lambda_2 \tilde{d}_v^T \tilde{d}_v - \frac{\lambda_3}{2} \tilde{\beta}^2 + \frac{\lambda_3}{2} \beta^2 \\ &\leq -\min\{4\lambda_2, \lambda_3\} \left(\frac{1}{2} \tilde{d}_v^T \tilde{d}_v + \frac{1}{2} \tilde{\beta}^2 \right) + \delta_0 \\ &\leq -\lambda_{\min} L_2 + \delta_0 \end{aligned} \quad (17)$$

where $\lambda_{\min} = \min\{4\lambda_2, \lambda_3\}$, $\delta_0 = \frac{\lambda_3}{2} \beta^2$, and one can obtain $0 \leq L_2 \leq \frac{\delta_0}{\lambda_{\min}} + \left[L_2(0) - \frac{\delta_0}{\lambda_{\min}} \right] \exp(-\lambda_{\min} t)$. According

to lemma 2, it is proved that the approximation error is exponentially convergent.

Remark 1: From Eq. (12) it can be noticed that the ASMDOB has the ability of filtering, so the high-frequency oscillation caused by $\text{sgn}(s)$ can be eliminated by itself.

B. Design of kinematic controller with prescribed performance

Define $e = q - q_d$ as the trajectory tracking error, where $q_d = [x_d \ y_d \ \varphi]^T$ presents the desired trajectory and φ is an auxiliary variable which will be introduced in the following parts. According to the kinematics model, one has

$$\dot{e} = Tu + d_v - \dot{q}_d. \quad (18)$$

To improve transient response characteristics and steady-state tracking accuracy, a performance function $\rho(t)$ is introduced which makes the tracking error satisfying

$$-\epsilon_i \rho_i(t) < e_i(t) < \epsilon_i \rho_i(t) \quad (19)$$

where e_i , ($i = 1, 2, 3$) denotes i th element in e , $0 < \epsilon_i \leq 1$ is a design constant, $\rho_i(t)$ is chosen as $\rho_i(t) = (\rho_{i0} - \rho_{i\infty}) \exp(-k_\rho t) + \rho_{i\infty}$ with $\rho_{i0} > \rho_{i\infty} > 0$ and $k_\rho > 0$.

Then define

$$\eta_i = \frac{1}{2} \ln \frac{\epsilon_i \rho_i(t) + e_i}{\epsilon_i \rho_i(t) - e_i} \quad (20)$$

as the i th element of transformed error η . The dynamics of the transformed error can be obtained as

$$\dot{\eta} = \Phi + \Lambda(Tu + d_v - \dot{q}_d) \quad (21)$$

where $\Phi = [\phi_1 \ \phi_2 \ \phi_3]^T$ with $\phi_i = -\frac{\epsilon_i \dot{\rho}_i(t) e_i}{\epsilon_i^2 \rho_i^2(t) - e_i^2}$, and $\Lambda = \text{diag}\{\Lambda_1 \ \Lambda_2 \ \Lambda_3\}$ with $\Lambda_i = \frac{\epsilon_i}{\epsilon_i^2 \rho_i^2(t) - e_i^2}$.

According to Eq. (1), the desired trajectory can be obtained as

$$\begin{cases} \dot{x}_d = v \cos \theta_d \\ \dot{y}_d = v \sin \theta_d \end{cases} \quad (22)$$

As coordinates x_d , y_d and the desired direction angle θ_d are not independent with each other, (x_d, y_d) is chosen as the target instruction. Then the controller is derived using backstepping technique as follows.

Step 1: Introducing the auxiliary control variable φ , and according to the kinematics model (1), define

$$\begin{cases} \dot{x} = v \cos \varphi + d_{v1} \\ \dot{y} = v \sin \varphi + d_{v2} \end{cases} \quad (23)$$

where d_{vi} , ($i = 1, 2, 3$) denotes i th element in d_v . Define a Lyapunov function candidate as

$$V_1 = \frac{1}{2} \eta_1^2 + \frac{1}{2} \eta_2^2. \quad (24)$$

Differentiating V_1 with respect to time, we have

$$\begin{aligned} \dot{V}_1 &= \eta_1 [\phi_1 + \Lambda_1 (v \cos \varphi + d_{v1} - \dot{x}_d)] \\ &\quad + \eta_2 [\phi_2 + \Lambda_2 (v \sin \varphi + d_{v2} - \dot{y}_d)]. \end{aligned} \quad (25)$$

Define

$$v \cos \varphi = \dot{x}_d + \Lambda_1^{-1}[-\phi_1 - k_1\eta_1 - k_2\text{sgn}^p(\eta_1) - k_3\text{sgn}(\eta_1)] - \hat{d}_{v1} \quad (26a)$$

$$v \sin \varphi = \dot{y}_d + \Lambda_2^{-1}[-\phi_2 - k_1\eta_2 - k_2\text{sgn}^p(\eta_2) - k_3\text{sgn}(\eta_2)] - \hat{d}_{v2} \quad (26b)$$

where k_1 , k_2 and k_3 are design parameters, \hat{d}_{vi} , ($i = 1, 2, 3$) is the i th element in \hat{d}_v and $0 < p < 1$. Substituting (26) into Eq. (25), one can obtain

$$\begin{aligned} \dot{V}_1 &= \eta_1[-k_1\eta_1 - k_2\text{sgn}^p(\eta_1) - k_3\text{sgn}(\eta_1) + \tilde{d}_{v1}] \\ &+ \eta_2[-k_1\eta_2 - k_2\text{sgn}^p(\eta_2) - k_3\text{sgn}(\eta_2) + \tilde{d}_{v2}] \\ &= -k_1\eta_1^2 - k_2\eta_1\text{sgn}^p(\eta_1) - k_3\eta_1\text{sgn}(\eta_1) + \eta_1\tilde{d}_{v1} \\ &- k_1\eta_2^2 - k_2\eta_2\text{sgn}^p(\eta_2) - k_3\eta_2\text{sgn}(\eta_2) + \eta_2\tilde{d}_{v2}. \end{aligned} \quad (27)$$

It can be noticed that while the value of k_3 is designed larger than $\max\{\tilde{d}_{v1}, \tilde{d}_{v2}\}$, one can obtain

$$\begin{aligned} \dot{V}_1 &\leq -k_1\eta_1^2 - k_2|\eta_1|^{1+p} - k_1\eta_2^2 - k_2|\eta_2|^{1+p} \\ &\leq -2k_1V_1 - 2k_2V_1^{(1+p)/2}. \end{aligned} \quad (28)$$

According to lemma 1, it can be concluded that η_1 and η_2 will converge to the equilibrium point in finite time. Let

$$m_1 = \dot{x}_d + \Lambda_1^{-1}[-\phi_1 - k_1\eta_1 - k_2\text{sgn}^p(\eta_1) - k_3\text{sgn}(\eta_1)] - \hat{d}_{v1} \quad (29a)$$

$$m_2 = \dot{y}_d + \Lambda_2^{-1}[-\phi_2 - k_1\eta_2 - k_2\text{sgn}^p(\eta_2) - k_3\text{sgn}(\eta_2)] - \hat{d}_{v2}. \quad (29b)$$

While the linear velocity and virtual control law is given by

$$v = \sqrt{m_1^2 + m_2^2} \quad (30a)$$

$$\varphi = \arctan \frac{m_2}{m_1} \quad (30b)$$

Eq. (26) can be guaranteed. From Eq. (30b), it can be seen that while ε_1 , ρ_1 are selected equal to ε_2 , ρ_2 , and the lumped disturbances are well observed, φ will converge to θ_d . To make θ track φ fast and effectively, the following step is proposed.

Step 2: Define the Lyapunov function as

$$V_2 = V_1 + \frac{1}{2}\eta_3^2. \quad (31)$$

Differentiating V_2 with respect to time and considering (27), one has

$$\begin{aligned} \dot{V}_2 &\leq -k_1\eta_1^2 - k_2\eta_1\text{sgn}^p(\eta_1) - k_1\eta_2^2 - k_2\eta_2\text{sgn}^p(\eta_2) \\ &+ \eta_3[\phi_3 + \Lambda_3(\omega + d_{v3} - \dot{\varphi})]. \end{aligned} \quad (32)$$

Design the angular velocity control law as

$$\begin{aligned} \omega &= \dot{\varphi} - \hat{d}_{v3} + \Lambda_3^{-1}[-\phi_3 - k_1\eta_3 - k_2\text{sgn}^p(\eta_3) \\ &- k'_3\text{sgn}(\eta_3)]. \end{aligned} \quad (33)$$

Substituting (33) into Eq. (32) and select k'_3 larger than \tilde{d}_{v3} , one can obtain

$$\begin{aligned} \dot{V}_2 &\leq -k_1\eta_1^2 - k_2|\eta_1|^{1+p} - k_1\eta_2^2 - k_2|\eta_2|^{1+p} \\ &- k_1\eta_3^2 - k_2|\eta_3|^{1+p} \leq -2k_1V_2 - 2k_2V_2^{(1+p)/2}. \end{aligned} \quad (34)$$

Based on lemma 1, we can conclude that both η_1 , η_2 and η_3 will converge to the equilibrium point in finite time. Then the convergence of the whole system can be guaranteed.

IV. SIMULATION RESULTS

To validate the efficiency of the proposed control scheme, simulation comparisons with the mostly used PID and SMC controllers have been conducted. A circular shape target trajectory is selected as

$$x_r = \cos(t), y_r = \sin(t). \quad (35)$$

External disturbances are given by

$$\begin{cases} d_{v1} = 0.5 \sin(t) \\ d_{v2} = 0.5 \cos(t) + 0.1 \cos(t + \frac{\pi}{2}) \\ d_{v3} = 0.1 \end{cases} \quad (36)$$

It can be seen that both periodic and constant interference with high amplitude are considered. Tracking results of the circular trajectory is illustrated in Fig.(2). To demonstrate the superiority of the developed DOB, the commonly used extended disturbance observer (ESO) is utilized to make a comparison. Observation results based on the proposed ASMDOB and ESO are demonstrated in the Fig. (3). It can be seen in these figures that all the disturbances in the x , y and θ directions are well estimated. Moreover, from the comparison results it can be noticed that the proposed ASMDOB has faster convergence speed and higher estimation accuracy.

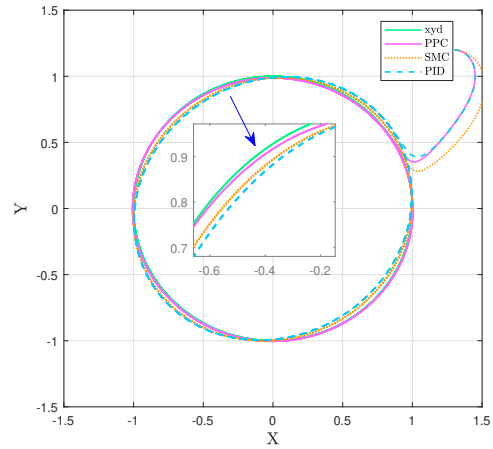


Fig. 2. Tracking results of the circular trajectory.

The tracking processes in x and y orientation as well as the linear and angular velocity are provided in Fig.(4). The starting point is set at (1.3, 1.2). To ensure the reliability

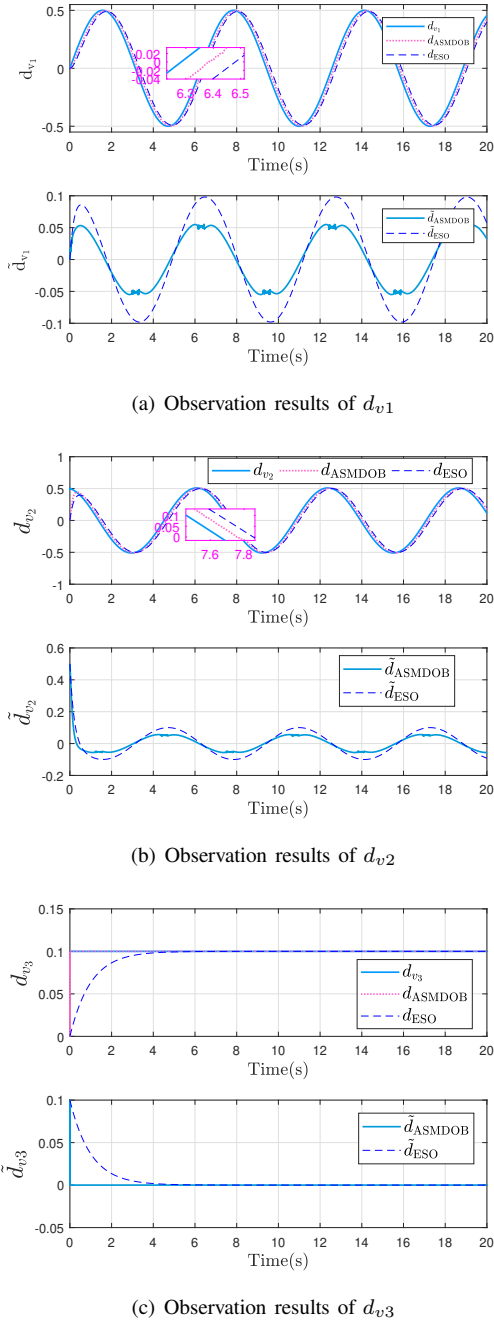


Fig. 3. Observation results of external disturbances.

of the comparison, the parameters of the controllers have been adjusted to their best performance. From these figures, it can be found that although the objective trajectory can be tracked with all these methods, the tracking performance is totally different. The tracking accuracy of the proposed PPC is obviously higher and the input is smoother than the traditional SMC. To provide a clearer comparison result, the tracking errors are shown in the Fig. (5), and the root mean square error (RMS) value, maximum (MAX) value, and the mean value of the errors are given in the Table I (unit: m).

Exactly, while the system converges, the tracking accuracy of PPC is kept within 0.01 m, which is much lower than that of similar controllers, and the box-plots of the tracking errors is given in Fig.(6). Therefore, it can be concluded that the proposed PPC could fully meet the control target of the ATRC.

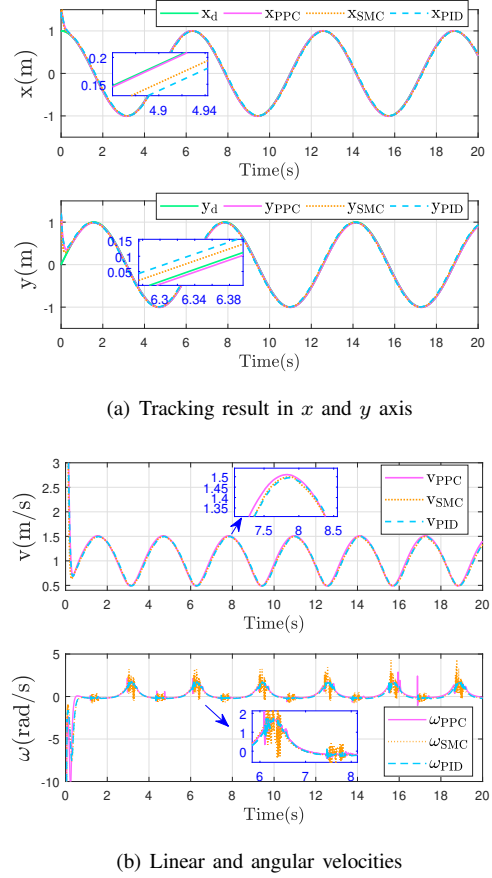


Fig. 4. Tracking results of the three controllers.

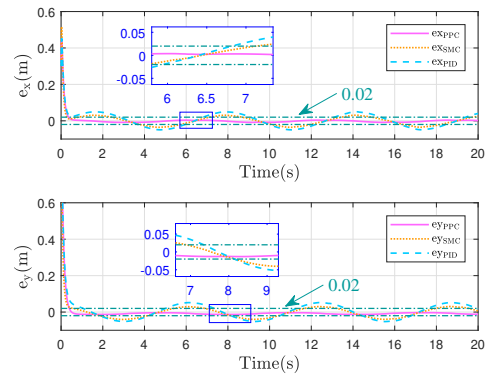


Fig. 5. Tracking errors of the three controllers.

TABLE I
COMPARISON OF THE TRACKING ERRORS.

Method	x-axis			y-axis		
	RMS	MAX	MEAN	RMS	MAX	MEAN
PPC	0.2236	0.4505	0.1371	0.6338	1.200	0.3812
SMC	0.2520	0.5170	0.1612	0.6368	1.200	0.3953
PID	0.2383	0.4522	0.1552	0.6683	1.200	0.4285

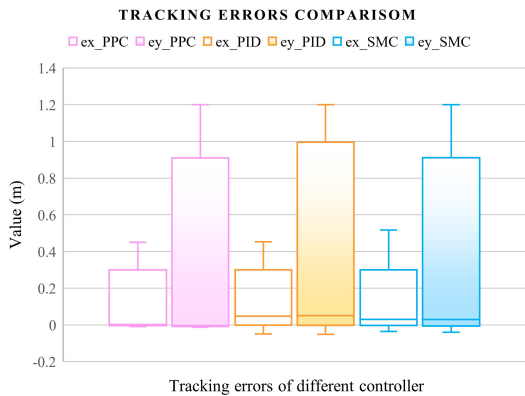


Fig. 6. Tracking error box-plots of the three controllers.

V. CONCLUSION AND FUTURE WORKS

This paper investigates an adaptive sliding mode disturbance observer based robust controller with prescribed performance for autonomous trolley collection mobile robots. To improve the engineering practicability, kinematics model is utilized and the disturbance observer is developed to guarantee the robustness. Prescribed performance control method integrated with backstepping technique is adopted to generate the control input, and in such manner both the stable and transient performance are guaranteed. In the future work, experiments will be conducted on the real robot platform to test the reliability of the proposed control scheme.

REFERENCES

- [1] J. Wang and M. Q.-H. Meng, "Real-time decision making and path planning for robotic autonomous luggage trolley collection at airports," *IEEE Transactions on Systems, Man, and Cybernetics: Systems*, vol. 52, no. 4, pp. 2174–2183, 2021.
- [2] A. Xiao, H. Luan, Z. Zhao, Y. Hong, J. Zhao, W. Chen, J. Wang, and M. Q.-H. Meng, "Robotic autonomous trolley collection with progressive perception and nonlinear model predictive control," in *2022 International Conference on Robotics and Automation (ICRA)*. IEEE, 2022, pp. 4480–4486.
- [3] J. Pan, X. Mai, C. Wang, Z. Min, J. Wang, H. Cheng, T. Li, E. Lyu, L. Liu, and M. Q.-H. Meng, "A searching space constrained partial to full registration approach with applications in airport trolley deployment robot," *IEEE Sensors Journal*, vol. 21, no. 10, pp. 11 946–11 960, 2020.
- [4] C. Wang, X. Mai, D. Ho, T. Liu, C. Li, J. Pan, and M. Q.-H. Meng, "Coarse-to-fine visual object catching strategy applied in autonomous airport baggage trolley collection," *IEEE Sensors Journal*, vol. 21, no. 10, pp. 11 844–11 857, 2020.
- [5] I. Matraji, A. Al-Durra, A. Haryono, K. Al-Wahedi, and M. Abou-Khousa, "Trajectory tracking control of skid-steered mobile robot based on adaptive second order sliding mode control," *Control Engineering Practice*, vol. 72, no. MAR., pp. 167–176, 2018.
- [6] G. Huskić, S. Buck, M. Herrb, S. Lacroix, and A. Zell, "High-speed path following control of skid-steered vehicles," *The International Journal of Robotics Research*, vol. 38, no. 9, pp. 1124–1148, 2019.
- [7] X. Yue, J. Chen, Y. Li, R. Zou, Z. Sun, X. Cao, and S. Zhang, "Path tracking control of skid-steered mobile robot on the slope based on fuzzy system and model predictive control," *International Journal of Control, Automation and Systems*, vol. 20, no. 4, pp. 1365–1376, 2022.
- [8] R. Xi and L. Tang, "Tracking control of a skid steered mobile robot with adaptive robust second order sliding-mode controller," in *2019 IEEE International Conference on Industrial Engineering and Engineering Management (IEEM)*. IEEE, 2019, pp. 293–297.
- [9] M. Chen, "Disturbance attenuation tracking control for wheeled mobile robots with skidding and slipping," *IEEE Transactions on Industrial Electronics*, vol. 64, no. 4, pp. 3359–3368, 2016.
- [10] H.-S. Kang, C.-H. Hyun, and S. Kim, "Robust tracking control using fuzzy disturbance observer for wheeled mobile robots with skidding and slipping," *International Journal of Advanced Robotic Systems*, vol. 11, no. 5, p. 75, 2014.
- [11] J. Lu, Y. Liu, W. Huang, K. Bi, Y. Zhu, and Q. Fan, "Robust control strategy of gradient magnetic drive for microrobots based on extended state observer," *Cyborg and Bionic Systems*, 2022.
- [12] L. Yu, J. Huang, and S. Fei, "Robust switching control of the direct-drive servo control systems based on disturbance observer for switching gain reduction," *IEEE Transactions on Circuits and Systems II: Express Briefs*, vol. 66, no. 8, pp. 1366–1370, 2018.
- [13] R.-D. Xi, T.-N. Ma, X. Xiao, and Z.-X. Yang, "Design and implementation of an adaptive neural network observer-based backstepping sliding mode controller for robot manipulators," *Transactions of the Institute of Measurement and Control*, vol. 0, no. 0, p. 0, 2023.
- [14] R. Xi, Z. Yang, and X. Xiao, "Adaptive neural network observer based pid-backstepping terminal sliding mode control for robot manipulators," in *2020 IEEE/ASME International Conference on Advanced Intelligent Mechatronics (AIM)*. IEEE, 2020, pp. 209–214.
- [15] W.-H. Chen, J. Yang, L. Guo, and S. Li, "Disturbance-observer-based control and related methods—An overview," *IEEE Transactions on Industrial Electronics*, vol. 63, no. 2, pp. 1083–1095, 2015.
- [16] S. Liang, R. Xi, X. Xiao, and Z. Yang, "Adaptive sliding mode disturbance observer and deep reinforcement learning based motion control for micropositioners," *Micromachines*, vol. 13, no. 3, p. 458, 2022.
- [17] H. Rabiee, M. Ataei, and M. Ekramian, "Continuous nonsingular terminal sliding mode control based on adaptive sliding mode disturbance observer for uncertain nonlinear systems," *Automatica*, vol. 109, p. 108515, 2019.
- [18] Y. Zhu, J. Qiao, and L. Guo, "Adaptive sliding mode disturbance observer-based composite control with prescribed performance of space manipulators for target capturing," *IEEE Transactions on Industrial Electronics*, vol. 66, no. 3, pp. 1973–1983, 2018.
- [19] D. Shi, J. Zhang, Z. Sun, and Y. Xia, "Adaptive sliding mode disturbance observer-based composite trajectory tracking control for robot manipulator with prescribed performance," *Nonlinear Dynamics*, vol. 109, no. 4, pp. 2693–2704, 2022.
- [20] R.-D. Xi, X. Xiao, T.-N. Ma, and Z.-X. Yang, "Adaptive sliding mode disturbance observer based robust control for robot manipulators towards assembly assistance," *IEEE Robotics and Automation Letters*, vol. 7, no. 3, pp. 6139–6146, 2022.
- [21] C. P. Bechlioulis and G. A. Rovithakis, "Adaptive control with guaranteed transient and steady state tracking error bounds for strict feedback systems," *Automatica*, vol. 45, no. 2, pp. 532–538, 2009.
- [22] F. Cheng, B. Niu, L. Zhang, and Z. Chen, "Prescribed performance-based low-computation adaptive tracking control for uncertain nonlinear systems with periodic disturbances," *IEEE Transactions on Circuits and Systems II: Express Briefs*, vol. 69, no. 11, pp. 4414–4418, 2022.
- [23] H. Wang, M. Li, C. Zhang, and X. Shao, "Event-based prescribed performance control for dynamic positioning vessels," *IEEE Transactions on Circuits and Systems II: Express Briefs*, vol. 68, no. 7, pp. 2548–2552, 2021.
- [24] Y.-S. Lu, "Sliding-mode disturbance observer with switching-gain adaptation and its application to optical disk drives," *IEEE Transactions on Industrial Electronics*, vol. 56, no. 9, pp. 3743–3750, 2009.